Inorg. Chem. **2005**, *44*, 9823–9828

A Kinetically Controlled Trans Bifunctionalized Organoimido Derivative of the Lindqvist-Type Hexamolybdate: Synthesis, Spectroscopic Characterization, and Crystal Structure of (n-$Bu_4N)_2\{trans\text{-}[Mo_6O_{17}(NAr)_2]\}$ (Ar = 2,6-dimethylphenyl)

Yun Xia,[†] Yongge Wei,*[,‡,§] Yuan Wang,[§] and Hongyou Guo*[,†]

Department of Chemistry, Beijing University of Chemical Technology, Beijing 100029, People's Republic of China, Department of Chemistry, Tsinghua University, Beijing 100084, People's Republic of China, and Department of Chemistry, State Key Laboratory for Structural Chemistry of Unstable and Stable Species, College of Chemistry and Molecular Engineering, Peking University, Beijing 100871, People's Republic of China

Received August 3, 2005

A kinetically controlled trans bifunctionalized organoimido derivative of hexamolybdate, (n-$Bu_4N)_2\{$trans-$[Mo_6O_{17}(NAr)_2]\}$ (Ar = 2,6-dimethylphenyl) **1**, in which the two 2,6-dimethylphenylimido groups are bonded to hexamolybdate at the trans positions, has been successfully synthesized in ca. 60% yield under mild reaction conditions. Its trans structure has been confirmed by a single-crystal X-ray diffraction study. In the crystals, cluster anions of **1** self-assemble into a 3D netlike structure via two different kinds of C–H···O hydrogen bondings, in which 1D supramolecular rectangular channels containing tetrabutylammonium cations form along the *a* axis. Compound **1** has also been characterized by ^{1}H NMR, IR, and UV–vis spectroscopic studies. UV–vis–near-IR reflectance spectroscopy measurements reveal the compound's nature of semiconductivity with an optical energy gap of 2.55 eV.

Introduction

A knowledge of the linking rules of selected building blocks allows for the generation of an enormous variety of structures, especially when a set of gradually differing building units is available. Of utmost importance is that these basic units can be linked to larger fragments, which can again react in subsequent processes in different ways.[1a] The organoimido derivatives of Lindqvist-type polyoxometalates (POMs),[1b] $[M_6O_{19}]^{n-}$, are a unique class of building blocks that are very suitable for this purpose because a Lindqvist ion has a superoctahedral structure approach to the O_h point group and the ion features its six terminal metal−oxo groups aligned along the Cartesian axes. Essentially, one or even all six terminal oxo groups of a Lindqvist ion could be replaced with various organoimido ligands, including aromatic amine iodides.[2] The chemistry field of organoimido derivatives of Lindqvist-type POMs has expanded quickly since E. A. Maatta pioneered this field about 15 years ago.[3] For example, a number of organoimido derivatives of the hexamolybdate ion $[Mo_6O_{19}]^{2-}$,[4] the pentatungstenmolybdate ion $[MoW_5O_{19}]^{2-}$,[5] and the hexatungstate ion $[W_6O_{19}]^{2-}$ [6] have been synthesized. Moreover, iodo- and ethynyl-functionalized phenylimido hexamolybdates have recently been discovered that can undergo Pd-catalyzed carbon−carbon coupling reactions,[7a] which has successfully been exploited to assemble hybrid nanodumbbells[7b] and polymers[8] in a more controllable manner.

* To whom correspondence should be addressed. Telephone: 86-10-62797852. E-mail: yonggewei@tsinghua.edu.cn (Y.W.), guohy@mail.buct.edu.cn (H.G.).
† Beijing University of Chemical Technology.
‡ Tsinghua University.
§ Peking University.

(1) (a) Ball, P. *Nature* **1998**, *395*, 745. (b) Proust, A.; Villanneau, R.; Delmont, R.; Artero, V.; Gouzerh, P. In *Polyoxometalate Chemistry: From Topology via Self-Assembly to Applications*; Kluwer: Dordrecht, The Netherlands, 2001.
(2) Peng, Z. H. *Angew. Chem., Int. Ed.* **2004**, *43*, 930.
(3) Du, Y.; Rheingold, A. L.; Maatta, E. A. *J. Am. Chem. Soc.* **1992**, *114*, 345.
(4) Strong, J. B.; Yap, G. P. A.; Ostrander, R.; Liable-Sands, L. M.; Rheingold, A. L.; Thouvenot, R.; Gouzerh, P.; Maatta, E. A. *J. Am. Chem. Soc.* **2000**, *122*, 639.
(5) Wei, Y. G.; Meng, L.; Cheung, C. F.-C.; Barnes, C. L.; Peng, Z. H. *Inorg. Chem.* **2001**, *40*, 5489.
(6) Mohs, T. R.; Yap, G. P. A.; Rheingold, A. L.; Maatta, E. A. *Inorg. Chem.* **1995**, *34*, 9.

10.1021/ic051319t CCC: $30.25
Published on Web 12/01/2005

Among organoimido derivatives of Lindqvist-type POMs, the bifunctionalized ones are potential building blocks for constructing POM-based hybrids, including nanotrimers, nanocircles, and even polymers.[2,8] It is obvious there are two geometric isomers for a terminal bifunctionalized organoimido derivative of a Lindqvist-type homo-POM, i.e., the cis and trans isomers. On the basis of the consideration of steric repulsion, one can imagine that the trans isomer is easy to synthesize and should be more familiar than the cis one. However, contrary to this common expectation, almost all the bifunctionalized Lindquist hexamolybdate derivatives reported in the literature prefer the cis structure to the trans structure,[4,8−10] and only one example of the trans bifunctionalized organoimido hexamolybdate was mentioned previously in the literature, as a brief communication and without reliable yield.[11] The synthesis of the trans isomer is still a challenge in the chemistry of organoimido derivatives of Lindqvist-type POMs. Recently, we and our co-workers at University of Missouri−Kansas City have developed a useful DCC dehydrating protocol for preparing the organoimido derivations of POMs.[5,8a,10b,12] Using this protocol, we now find that the trans isomer of a bifunctionalized derivative, *trans*-$[Mo_6O_{17}(NAr)_2]^{2-}$ (Ar = 2,6-dimethylphenyl) **1**, can be prepared conveniently with good yield under supporting conditions. In this paper, we report the detailed synthesis and structural characterization of the trans derivative **1** and its features that are different from those of the corresponding cis isomer **2**.

Experimental Section

Materials and General Methods. All chemicals purchased were of analytical grade, and were used without further purification, except for acetonitrile, which was dried by refluxing in the presence of CaH_2 and distilled prior to use. $(n\text{-}Bu_4N)_2Mo_6O_{19}$ was synthesized by an improved method of the literature procedure,[13] recrystallized from anhydrous acetone, and dried under vacuum before use. IR spectra were recorded in KBr pellets with a Bruker FT-IR VECTOR 22 spectrophotometer. UV−vis absorption spectra were recorded in acetonitrile solutions with a Shimadzu UV-2501PC spectrophotometer. ^{1}H NMR spectra were recorded at 600.13 MHz at 298 K using a Bruker AV-600 instrument. Optical diffuse reflectance spectra were performed on a Shimadzu UV-3100 recording spectrophotometer with a Φ60 mm integrating sphere from 250 to 2500 nm at room temperature. Initially, the 100% line flatness of the spectrophotometer was set using barium sulfate ($BaSO_4$). A powder sample of the compound was mounted on the sample holder. The thickness of the sample was approximately 2.00 mm, which was much larger than the size of the individual crystal particles.[14]

Synthesis of 1. To a 100 mL round-bottom flask were added anhydrous acetonitrile (50 mL), 2,6-dimethylaniline (0.25 mL, 2.0 mmol), $(n\text{-}Bu_4N)_2Mo_6O_{19}$ (1.36 g, 1.0 mmol), and DCC (1,3-dicyclohexylcarbodiimide) (0.43 g, 2.1 mmol). The solution was warmed in an oil bath with a heating mantle, and was stirred mechanically. The reaction mixture was brought to reflux, and was held at the refluxing temperature of 95 °C for 12 h. The reaction mixture was then cooled to room temperature, and was allowed to stand for 2 h until a white precipitate of 1,3-dicyclohexylurea formed. The reaction mixture was gravitationally filtered to remove 1, 3-dicyclohexylurea and other insoluble materials. The resulting filtrate was evaporated to give red viscous oil, and was then washed with ethanol. The residue was resolved in 60 mL of acetonitrile. After the addition of 20 mL of ethanol to this red solution, the crude product was obtained on evaporation as red block crystals of **1** within 3 days (yield: ca. 60% based on Mo). X-ray quality single crystals were grown in a test tube by slow diffusion of the carefully layered-on ethanol into an acetone and acetonitrile solution of the crude product. ***trans*-$C_{48}H_{90}Mo_6N_4O_{17}$.** Anal. Calcd: C, 36.70; H, 5.77; N, 3.57. Found: C, 36.73; H, 5.74; N, 3.61. IR (KBr): $\tilde{\nu}_{max}$ 991 (m), 944 (s) [ν(Mo═N, Mo═O)], 807 (s), 739 (s) cm^{-1} [ν(MoOMo)]. ^{1}H NMR (CD_3CN): δ 7.07 (d, C_6H_3(m), 4H), 6.92 (t, C_6H_3(p), 2H), 3.10 (t, NCH_2, 16H), 2.63 (s, *(Ar-)Me*$_2$, 12H), 1.61 (m, CH_2, 16H), 1.36 (m, CH_2, 16H), 0.98 (t, CH_3, 24H). UV−vis (MeCN): λ_{max} 245, 358 nm. ***cis*-$C_{48}H_{90}Mo_6N_4O_{17}$.**[8a] Anal. Calcd: C, 36.70; H, 5.77; N, 3.57. Found: C, 36.86; H, 5.80; N, 3.24. IR (KBr): $\tilde{\nu}_{max}$ 961 (m), 944 (s) [ν(Mo═N, Mo═O)]. ^{1}H NMR (CD_3CN): δ 7.06 (d, C_6H_3(m), 4H), 6.90 (t, C_6H_3(p), 2H), 3.10 (t, NCH_2, 16H), 2.62 (s, *(Ar-)Me*$_2$,12H), 1.63 (m, CH_2, 16H), 1.37 (m, CH_2, 16H), 0.99 (t, CH_3, 24H). UV−vis (MeCN): λ_{max} 245, 354 nm.

X-ray Crystallography. X-ray single-crystal diffraction data for a red prism crystal of **1** with dimensions of 1.0 × 0.70 × 0.35 mm^3 were collected on a Bruker Smart Apex CCD diffractometer with graphite-monochromatized Mo Kα radiation (λ = 0.71073 Å) at room temperature (293 ± 2 K) in the range of 2.32° < θ < 27.48°. A total of 23 152 reflections were measured, of which there were 7036 unique reflections and 6257 observed reflections with the criterion of $I \geq 2\sigma(I)$. The raw data were corrected for LP factors and empirical absorption. The structure was solved by the direct method, and was refined anisotropically by full-matrix least squares on F^2. The computations were performed using the SHELX97 program.[15] All the drawings were generated with the XP program in the SHELXTL software package, version 5.01.[16]

Results and Discussion

Structure Description. A summary of X-ray crystal data for compound **1** is presented in Table 1, and selected bond lengths and angles are given in Table 2. An ORTEP diagram of the cluster anion is shown in Figure 1. As it is shown,

(7) (a) Xu, B.; Wei, Y. G.; Barnes, C. L.; Peng, Z. *Angew. Chem., Int. Ed.* **2001**, *40*, 2290. (b) Lu, M.; Wei, Y. G.; Xu, B.; Cheung, C. F.-C.; Peng, Z.; Powell, D. R. *Angew. Chem., Int. Ed.* **2002**, *41*, 1566.

(8) (a) Xu, L.; Lu, M.; Xu, B.; Wei, Y. G.; Peng, Z.; Powell, D. R. *Angew. Chem., Int. Ed.* **2002**, *41*, 4129. (b) Lu, M.; Xie, B.; Kang, J.; Chen, F.-C.; Yang, Y.; Peng, Z. H. *Chem. Mater.* **2005**, *17*, 402.

(9) Strong, J. B.; Ostrander, R.; Rheingold, A. L.; Maatta, E. A. *J. Am. Chem. Soc.* **1994**, *116*, 3601.

(10) (a) Li, Q.; Wu, P. F.; Wei, Y. G.; Wang, Y.; Wang, P.; Guo, H. Y. *Inorg. Chem. Commun.* **2004**, *7*, 524. (b) Li, Q.; Wu, P. F.; Wei, Y. G.; Xia, Y.; Wang, Y.; Guo, H. Y. *Z. Anorg. Allg. Chem.* **2005**, *631*, 773.

(11) (a) Clegg, W.; Errington, R. J.; Fraser, K. A.; Holmes, S. A.; Schäfer, A. *Chem. Commun.* **1995**, 455. (b) A new example, found after this paper was submitted, that was mentioned by one of the reviewers: Qin, C.; Wang, X. L.; Xu, L.; Wei, Y. G. *Inorg. Chem. Commun.* **2005**, *8*, 751.

(12) Wei, Y. G.; Xu, B. B.; Barnes, C. L.; Peng, Z. H. *J. Am. Chem. Soc.* **2001**, *123*, 4083. (b) Wu, P. F.; Li, Q.; Ge, N.; Wei, Y. G.; Wang, Y.; Wang, P.; Guo, H. Y. *Eur. J. Inorg. Chem.* **2004**, 2819.

(13) Hur, N. H.; Klemperer, W. G.; Wang, R.-C. *Inorg. Synth.* **1990**, *27*, 77.

(14) McCarthy, T. J.; Ngeyi, S. P.; Liao, J. H.; DeGroot, D. C.; Hogan, T.; Kannewurf, C. R.; Kanatzidis, M. G. *Chem. Mater.* **1993**, *5*, 331.

(15) Sheldrick, G. M. *SHELX-97*: *program for structure refinement*; University of Göttingen: Göttingen, Germany, 1997.

(16) Sheldrick, G. M. *SHELXTL*, *version 5.10*, *Structure Determination Software Suite*; Bruker AXS: Madison, WI, 1998.

Table 1. Crystal Data and Structure Refinement for Compound **1**

empirical formula	$C_{48}H_{90}Mo_6N_4O_{17}$
fw	1570.88
T (K)	293(2)
wavelength (Å)	0.71073
cryst syst	monoclinic
space group	$P2_1/n$
a (Å)	11.0358(17)
b (Å)	16.569(3)
c (Å)	17.507(3)
α (deg)	90
β (deg)	105.377(2)
γ (deg)	90
V (Å^3)	3086.5(8)
Z	2
D_c (mg m^{-3})	1.690
μ (mm^{-1})	1.247
F(000)	1588
cryst size (mm^3)	1.00 × 0.70 × 0.35
θ range for data collection	2.32−27.48°
index ranges	$-13 \le h \le 14$, $-21 \le k \le 21$, $-22 \le l \le 22$
no. of reflns collected/unique	23152/7036 [R(int) = 0.0229]
completeness to θ = 27.48° (%)	99.4
max. and min. transmission	0.6694 and 0.3687
refinement method	full-matrix least-squares on F^2
data/restraints/params	7036/0/337
GOF on F^2	1.059
final R indices [$I > 2\sigma(I)$]	R1 = 0.0329, wR2 = 0.0858
R indices (all data)	R1 = 0.0376, wR2 = 0.0900
largest diff. peak and hole (e Å^{-3})	1.233 and −0.650

Table 2. Selected Bond Lengths (Å) and Angles (deg) for Compound **1**

Mo1−N1	1.742(2)
Mo1−O9	1.896(2)
Mo1−O6	1.913(2)
Mo1−O4	1.978(2)
Mo1−O5	1.9806(19)
Mo1−O1	2.2579(3)
Mo2−O2	1.696(2)
Mo2−O5#1[a]	1.860(2)
Mo2−O7	1.896(2)
Mo2−O9	1.9450(19)
Mo2−O8	1.989(2)
Mo2−O1	2.3413(4)
Mo3−O3	1.694(2)
Mo3−O4#1	1.8783(19)
Mo3−O8#1	1.910(2)
Mo3−O6	1.933(2)
Mo3−O7	1.980(2)
Mo3−O1	2.3514(3)
N1−C1	1.383(3)
C1−N1−Mo1	170.4(2)
N1−Mo1−O9	104.55(11)
N1−Mo1−O6	103.73(10)
N1−Mo1−O4	100.23(10)
N1−Mo1−O5	99.73(11)
N1−Mo1−O1	175.69(9)
Mo1−O1−Mo1#1	180.000(8)
Mo1−O1−Mo2	89.764(12)
Mo1−O1−Mo2#1	90.236(12)
Mo1−O1−Mo3	89.746(14)
Mo1−O1−Mo3#1	90.254(14)
Mo2−O1−Mo3	89.885(10)
Mo2−O1−Mo2#1	180.000(10)
Mo2−O1−Mo3#1	90.115(10)
Mo(3)−O(1)−Mo(3)#1	180.000(11)

[a] Symmetry transformations used to generate equivalent atoms: #1 = $-x+1, -y+1, -z$.

the two 2,6-dimethylphenylimido ligands occupy two terminal positions in the trans fashion. The Mo−N bond

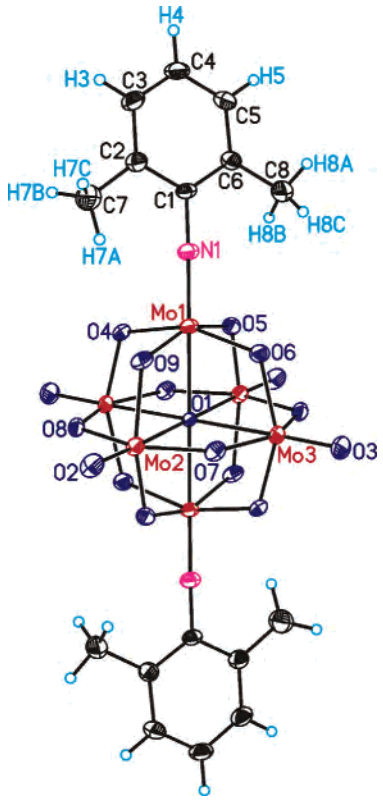

Figure 1. ORTEP drawing and atomic labeling scheme in an asymmetric unit of the cluster anion of **1**.

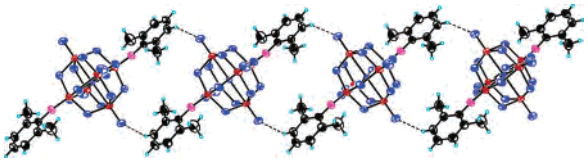

Figure 2. 1D hydrogen bonding chain assembled from cluster anions of **1**.

distances and the C−N−Mo bond angles are typical of organoimido groups bonded at an octahedral d^0 metal center, and are consistent with a substantial degree of M≡N triple-bond character.[17] But compared with those of **2**, the Mo−N bond distances (1.742 Å) of **1** are longer; the C−N−Mo bond angles (C1−N1−Mo1, 170.4°) of **1** are in the range of those in **2**. Compared to those of the hexamolybdate, the bond lengths of the other four terminal oxo groups of **1** do not vary appreciably. The Mo1−O1 and Mo1^i−O1 distances (symmetry code *i*: $1-x, 1-y, -z$), i.e., the distances between Mo atoms bearing imido groups and the central oxygen atom, are both significantly shorter than the other Mo−O1 distances.

There are interesting hydrogen bonding interactions among the cluster anions of **1**. Two pairs of parallel C−H···O hydrogen bonds (C5−H5···O3^{ii}, 3.396 Å, symmetry code *ii*: $-x, 1-y, -z$) between a cluster anion and its two neighbors arrange the cluster anions of **1** into 1D chain along the *a* axis (Figure 2). In the (1 0 1) plane, four C−H···O hydrogen bonds (C4−H4···O2^{iii}, 3.214 Å, symmetry code *iii*: $-1/2+x, 3/2-y, 1/2+z$) between a cluster anion and its

(17) Wigley, D. E. *Prog. Inorg. Chem.* **1992**, *31*, 239.

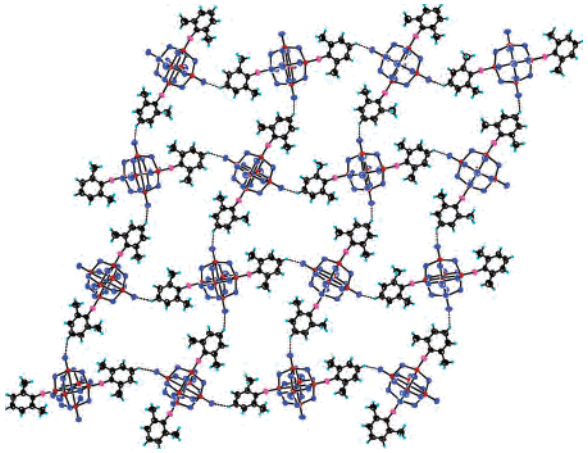

Figure 3. 2D netlike array of cluster anions of **1** via C−H···O hydrogen bonds.

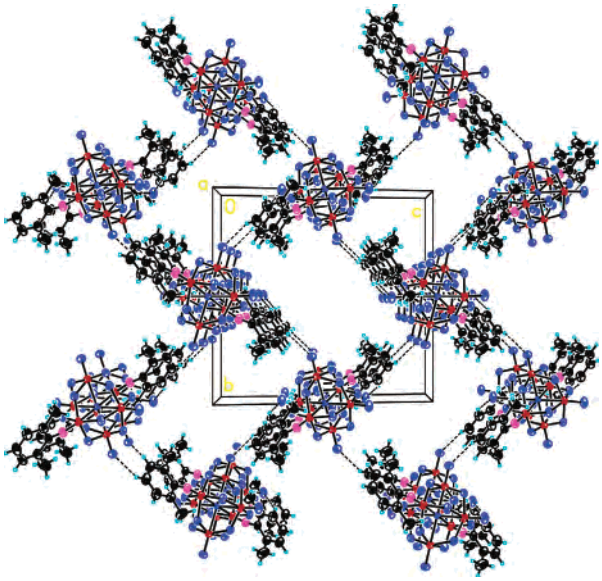

Figure 4. Packing view of cluster anions of **1**, which highlights rectangular 1D channels running through along the *a* axis.

four neighboring cluster anions result in a 2D netlike assembly of the cluster anions of **1** (Figure 3). Such nets are linked to each other along the *a* axis through pairs of parallel C5−H5···O3^{ii} hydrogen bonds, constructing the 3D array of cluster anions of **1**, where 1D supramolecular rectangular channels, parallel to the *a* axis, with a size of ca. 10.90 × 8.32 Å^2 (Figure 4) are formed, encapsulating the counter tetrabutylammonium cations.

In a word, the whole crystal structure of **1** is constructed by two different kinds of C−H···O hydrogen bonds, together with the electrostatic interactions between the counter tetrabutylammonium cations and cluster anions of **1**.

Preparation of the Compound. As shown in Scheme 1, the reaction of $(n\text{-}Bu_4N)_2Mo_6O_{19}$ with 2.0 equiv of 2,6-dimethylaniline at a lower temperature of 95 °C in the presence of the dehydrating agent, DCC, afforded a red block crystalline product of the trans derivative **1** in a good yield of 60%. As observed, there used to be trace amounts of mono- and cis-bifunctionalized imido derivatives formed if the reaction were not controlled carefully during this preparation, although these byproducts can be easily detected

Scheme 1. Synthesis of Trans and Cis Isomers **1** and **2,** respectively.

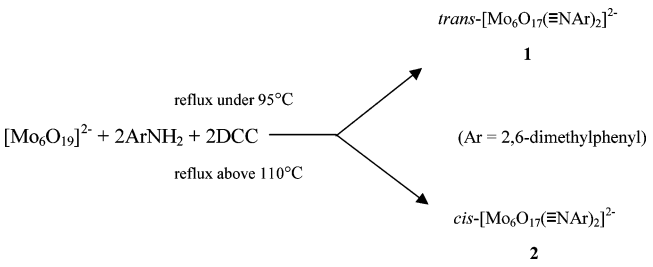

using ^{1}H NMR techniques, and can be removed by recrystallization. In addition, **1** also formed in the reaction of $(n\text{-}Bu_4N)_2Mo_6O_{19}$ with only 1.0 equiv of 2,6-dimethylaniline at a lower temperature but with a long refluxing time. However, when the reaction with the same reactant ratio proceeded at a higher refluxing temperature (in an oil bath warmer than 110 °C) and for a longer time, it was found that the yield of **1** was dramatically reduced, whereas that of the cis derivative **2** improved sharply. These observations imply that **1** is the kinetically controlled product whereas **2** is the thermodynamically favored one. Moreover, they also suggest that molybdyl groups have been activated in functionalized hexamolybdates, and that the molybdyl group trans to the imido group in a monosubstituted hexamolybdate is more reactive than the cis one.

Although both previous experiments and some theoretical studies[18] show that bifunctionalized hexamolybdate derivatives prefer to form cis rather than trans structures, our experiment proves that trans derivatives not only can be synthesized but also exist stably at room temperature. Although we need detailed theoretical studies to explain this fact, our result can also be expected if the following factors are taken into consideration. First, the formation of the trans structure has less steric repulsion than the cis one during organic substitution reactions, so that the trans terminal oxo group of a monosubstituted $[Mo_6O_{18}NR]^{2-}$ is more available to be attacked by the second ligand. Second, according to previous crystal structure studies and the resulting geometrical parameters[12,19] of hexamolybdate ion $[Mo_6O_{19}]^{2-}$ and its monosubstituted derivatives $[Mo_6O_{18}NR]^{2-}$, when an organoimido is introduced into $[Mo_6O_{19}]^{2-}$, the symmetry of $[Mo_6O_{18}NR]^{2-}$ is reduced from O_h to C_{2v}. In the meantime, the central oxygen atom is drawn closer to the imido-bearing Mo atom, and moves away from the Mo atom trans to the imido group, whereas the distances of the other four Mo−O_c bonds cis to the imido group hardly stay invariable, compared to that in $[Mo_6O_{19}]^{2-}$. As the central oxygen atom is the most negatively charged, it is reasonable to believe[18] that such a structural feature renders the Mo atom trans to the imido group the most positively charged in monosubstituted imido hexamolybdates, and is more reactive to being attacked by nucleophilic aromatic amines than the four cis Mo atoms. So the second arylimido group is easily introduced onto the trans site of monosubstituted hexamolybdates.

(18) Yan, L. K.; Su, Z. M.; Guan, W.; Zhang, M. *J. Phys. Chem. B* **2004**, *108*, 17337.
(19) Tytko, K. H.; Mehmke, J.; Fischer, S. *Struct. Bonding (Berlin)* **1999**, *93*, 129.

However, at higher reaction temperatures, presumably, the Mo atoms cis to the imido group also become reactive, and four such reactive sites increase the probability of the formation of the cis isomer. As for the preferred formation temperature for the trans and cis isomers of other arylimido hexamolybdates, it is still under study in our laboratory.

Spectroscopic Studies. IR Spectroscopy. In the low wavenumber region of the IR spectra ($\tilde{\nu} < 1000$ cm^{-1}), compound **1** displays a pattern characteristic of the Lindqvist structure. Actually, the IR bands of the aniline ligand in this region (mostly γ(C−C and C−H)) are of low intensity with respect to those of the polyoxometalate framework. Compound **1** presents more complex features than $(n\text{-}Bu_4N)_2[Mo_6O_{19}]$, especially in the 1000−700 cm^{-1} range characteristic of Mo−O stretching vibrations. In particular, the strong ν_{as}(Mo−O$_t$) band observed at 958 cm^{-1} in $(n\text{-}Bu_4N)_2[Mo_6O_{19}]$[20] splits into two more or less resolved bands ($\Delta\tilde{\nu} \approx 50$ cm^{-1}) in this arylimido derivative. In the approximation of separate Mo−O$_t$ and Mo−N vibrators, the stronger band, at low energy ($\tilde{\nu} \approx 944$ cm^{-1}), should be assigned to the ν_{as}(Mo−O$_t$) mode, whereas the less intense band ($\tilde{\nu} \approx 991$ cm^{-1}) might associate principally with the Mo−N vibration.[21−23a] Similarly, the broad and strong band observed at 797 cm^{-1} in the parent hexamolybdate, which was assigned to a Mo−O$_b$ stretching mode, also splits into two components ($\Delta\tilde{\nu} \approx 70$ cm^{-1}) in compound **1**. As observed, such a split is more obvious in compound **1** than in cis compound **2**, because compound **1** has a symmetry (D_{2h}) different than that of compound **2** (C_{2v}).

In other regions, compounds **1** and **2** have almost the same pattern characteristics. In the high-frequency region, the aromatic ν(Ar−H) bands ($\tilde{\nu} = 3058$ cm^{-1}) are hardly visible, due to their low intensity, and the complex pattern around 2900 cm^{-1} contains aliphatic ν(C−H) bands of both the tetrabutylammonium cation and the substituent on the aromatic ring. In the medium-frequency region (1650−1000 cm^{-1}), there are characteristic peaks from ν(C−N) and the 2,6-dimethylanilido group: the wide band in the region of 1639 cm^{-1}, 1585 cm^{-1}, and an acute band at 1465 cm^{-1} were shown to be associated with ν(C═C) of the benzene mode; 1380 cm^{-1} was assigned to δ(C−H) of the methyl group; 1317 and 1251 cm^{-1} were thought to be associated with ν-(C−N) of the arylimido group.

^{1}H NMR Spectroscopy. The ^{1}H NMR spectrum (in CD_3CN) of compound **1** shows clearly resolved signals, all of which can be unambiguously assigned. The integration matches well with the assumed structure. Signals at about 7.0 ppm are attributable to six protons of the aromatic group, and those at 2.63 ppm are attributable to the protons of two methyl groups on the benzene ring. But compared to the ^{1}H NMR spectrum of the corresponding free 2,6-dimethylaniline, the protons of aromatic and methyl groups exhibit significantly downfield chemical shifts, indicating the much weaker shielding nature of the $[Mo_5O_{18}-(M{\equiv}N^-)]^{2-}$ than the amino group NH_2. By comparing integral values of ligand resonances to integral values of the *n*-tetrabutylammonium ion resonances, we can easily quantify the extent of organoimido substitution, i.e., the ratio of ligand to hexamolybdate. In this way, we found that the ratio is approximately 2, consistent with compound **1** being the bifunctionalized product.

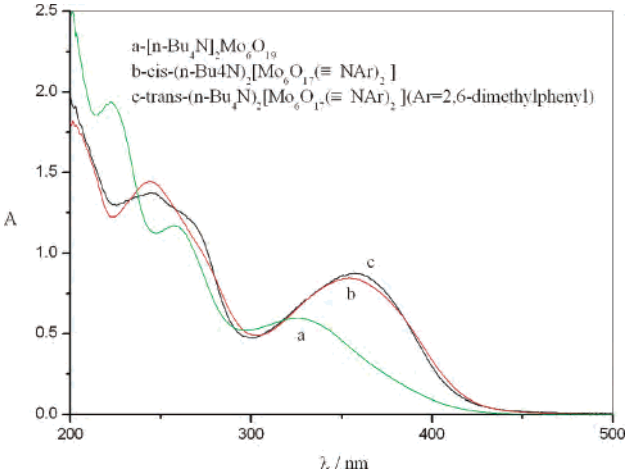

Figure 5. UV−vis absorption spectra of $[n\text{-}Bu_4N]_2[Mo_6O_{19}]$, compounds **1** and **2**.

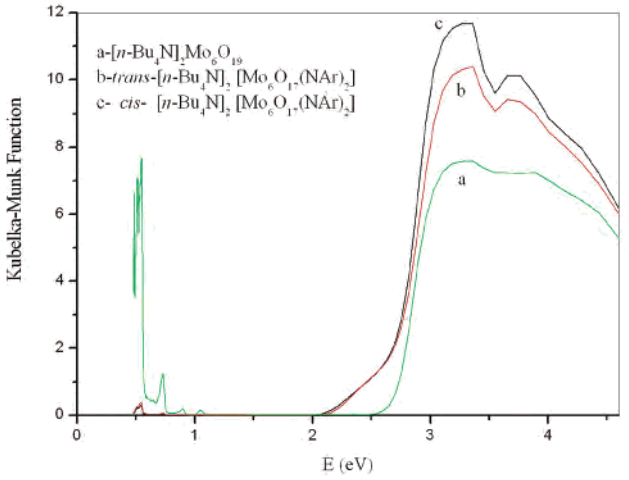

Figure 6. K−M function vs energy (eV) curve of $[n\text{-}Bu_4N]_2[Mo_6O_{19}]$, compounds **1** and **2**.

UV−Vis Spectroscopy. Figure 5 shows the UV−vis absorption spectra of the tetrabutylammonium salts of $[Mo_6O_{19}]^{2-}$, the two isomers **1** and **2**. The lowest-energy electronic transition at 325 nm in $[Mo_6O_{19}]^{2-}$ was assigned to a charge-transfer transition from the terminal oxygen nonbonding π-type HOMO to the molybdenum π-type LUMO, which is, in agreement with the literature, bathochromically shifted considerably, and became considerably more intense in **1** (358 nm) and **2** (354 nm), indicating that the Mo−N π-bond is formed in these organoimido derivatives.[23b] The larger red-shift in the trans isomer **1** than in

(20) Rocchiccioli-Deltcheff, C.; Thouvenot, R.; Fouassier, M. *Inorg. Chem.* **1982**, *21*, 30.
(21) Proust, A.; Thouvenot, R.; Chaussade, M.; Robert, F.; Gouzerh, P. *Inorg. Chim. Acta* **1994**, *224*, 81.
(22) Roesner, R. A.; McGrath, S. C.; Brockman, J. T.; Moll, J. D.; West, D. X.; Swearingen, J. K.; Castineiras, A. *Inorg. Chim. Acta* **2003**, *342*, 37.
(23) (a) Nugent, W.; Mayer, J. E. *Metal−Ligand Multiple Bonds*; Wiley: New York, 1988; pp 123−125. (b) Nugent, W.; Mayer, J. E. *Metal−Ligand Multiple Bonds*; Wiley: New York, 1988; p 112.

the cis isomer **2** is consistent with a longer and more effective conjugation in **1** than in **2**.

Optical Band Gap. To explore the potential conductivity of compounds, we used the measurement of diffuse reflectivity for a powder sample to obtain its band gap (E_g), which agrees rather well with that obtained by the absorption measurement from a single crystal.[24] The band gap (E_g) was determined as the intersection point between the energy axis and the line extrapolated from the linear portion of the absorption edge in a plot of the Kubelka−Munk function F against energy E.[25] The Kubelka−Munk function, $F = (1 - R)^2/2R$, was converted from the recorded diffuse reflectance data, where R is the reflectance of an infinitely thick layer at a given wavelength.[26] The F vs E plot, as shown in Figure 6, displays a steep absorption edge, from which E_g can be assessed: compound **1** is at 2.55 eV and compound **2** is at 2.6 eV. The reflectance spectrum measurement reveals the presence of an optical band gap and the nature of semiconductivity with a large energy gap for these two compounds. The E_g's of both **1** and **2** are smaller than that of the parent salt of $[Mo_6O_{19}]^{2-}$, which also indicates the formation of the Mo−N π-bond. And the data showing that E_g of **1** is a little lower than that of **2** show there is a more effective delocalization of π-electrons from the conjugated organoimido ligand to the metal oxygen cluster in compound **1**.

(24) (a) McCarthy, T. J.; Ngeyi, S. P.; Liao, J. H.; DeGreet, D. C.; Hogan, T.; Kannewurf, C. R.; Kanatzidis, M. G. *Chem. Mater.* **1993**, *5*, 331. (b) Li, J.; Chen, Z.; Wang, X. X.; Proserpio, D. M. *J. Alloys Compd.* **1997**, *262*−*263*, 28.

(25) Pankove, J. I. *Optical Processes in Semiconductors*; Prentice-Hall: Englewood Cliffs, NJ, 1971.

(26) Kortun, G. *Reflectance Spectroscopy*; Springer-Verlag: New York, 1969.

Conclusions

A trans bifunctionalized organoimido derivative of hexamolybdate, $(n\text{-}Bu_4N)_2\{trans\text{-}[Mo_6O_{17}(NAr)_2]\}$ (Ar = 2,6-dimethylphenyl) **1**, has been successfully synthesized by using $[Mo_6O_{19}]^{2-}$ as the starting cluster under mild reaction conditions with good yields. Unlike cis isomer **2**, which is thermodynamically favored, compound **1** is a kinetically controlled product. The molecular structure of **1** has been confirmed by a single-crystal X-ray diffraction study. In the crystals, the cluster anions form a 3D netlike structure with supramolecular rectangular channels via two different kinds of C−H···O hydrogen bonds. Compared to cis isomer **2**, compound **1** shows a stronger delocalization of π-electrons from the conjugated organoimido ligand to the metal oxygen cluster. Its nature of semiconductivity with a band gap of 2.55 eV has been substantiated by a solid UV−visible−near-IR reflectance spectroscopy measurement. The preparation of **1** with good yields opens a way for preparing other trans bifunctionalized imido derivatives of hexamolybdate, and is helpful for potential applications in constructing catenulate POM-based organic/inorganic hybrid molecular materials.

Acknowledgment. This work is sponsored by NFSC 20201001, SRF for ROCS of SEM, and MOST TG20000-77503.

Supporting Information Available: Listing of X-ray crystallographic data in CIF format. This material is available free of charge via the Internet at http://pubs.acs.org.

IC051319T